Analytical Biochemistry 542 (2018) 24–28

Contents lists available at ScienceDirect

Analytical Biochemistry

journal homepage: www.elsevier.com/locate/yabio

^{15}N CEST data and traditional model-free analysis capture fast internal dynamics of DJ-1

Jonathan Catazaro[a], Tessa Andrews[a], Nicole M. Milkovic[b], Jiusheng Lin[b], Austin J. Lowe[a], Mark A. Wilson[b], Robert Powers[a,c,*]

[a] Department of Chemistry, University of Nebraska-Lincoln, Lincoln, NE 68588-0304, USA
[b] Department of Biochemistry, University of Nebraska-Lincoln, Lincoln, NE 68588-0664, USA
[c] Nebraska Center for Integrated Biomolecular Communication, University of Nebraska-Lincoln, Lincoln, NE 68588-0304, USA

ARTICLE INFO

Keywords:
CEST
Protein dynamics
NMR
DJ-1

ABSTRACT

Previous studies have shown that relaxation parameters and fast protein dynamics can be quickly elucidated from ^{15}N-CEST experiments [1]. Longitudinal R_1 and transverse R_2 values were reliably derived from fitting of CEST profiles. Herein we show that ^{15}N-CEST experiments and traditional modelfree analysis provide the internal dynamics of three states of human protein DJ-1 at physiological temperature. The chemical exchange profiles show the absence of a minor state conformation and, in conjunction with ^{1}H-^{15}N NOEs, show increased mobility. R_1 and R_2 values remained relatively unchanged at the three naturally occurring oxidation states of DJ-1, but exhibit striking NOE differences. The NOE data was, therefore, essential in determining the internal motions of the DJ-1 proteins. To the authors' knowledge, we present the first study that combines ^{15}N CEST data with traditional model-free analyses in the study of a biological system and affirm that more 'lean' model-free approaches should be used cautiously.

Introduction

NMR spectroscopy is a powerful tool for the study of protein structures and dynamics in the solution state. Over the years, many NMR methods have been developed to observe protein dynamics for a range of timescales [2]. In which, fast timescale dynamics have been traditionally studied using two-dimensional (2D) ^{1}H-^{15}N HSQC R_1, R_2, and heteronuclear NOE experiments with the Carr-Purcell-Meiboom-Gill (CPMG) relaxation dispersion approach [3]. The T_1, T_2 and NOE data obtained from these experiments are routinely used to characterize sub-nano to millisecond protein dynamics with modelfree formalism [4,5]. The CPMG approach has also been extended to the study of conformational exchange due to its sensitivity to chemical shift differences between ground and excited states [6]. However, CPMG relaxation dispersion fails for proteins undergoing slow conformational exchange or for lowly populated excited states [7].

Recent advances employing saturation transfer, such as chemical exchange saturation transfer (CEST) and dark-state exchange saturation transfer (DEST), have enabled the detection of these previously invisible protein states [7,8]. Several studies have already reported the use of CEST to study the invisible conformers of slowly exchanging proteins on the millisecond to second timescale [1,9–12]. Additionally, the fitting of CEST profiles have been shown to reliably extract R_1 and R_2 parameters that can be used for modelfree analysis of fast timescale dynamics (ps to ns). Thus, the simultaneous measurement of both fast and slow timescale dynamics is possible with the CEST experiment. The extraction of the R_1 and R_2 parameters is particularly advantageous due to the fact that CEST and CPMG experiments can be acquired in a similar amount of experimental time [12]. To date, however, no study has combined CEST-derived R_1 and R_2 parameters with ^{1}H-^{15}N NOE data to establish the picosecond to nanosecond dynamics of a protein. Instead, leaner versions of modelfree have been applied without the NOE data [1].

The NOE is a sensitive measure of the high frequency motions as it reports directly on the structure of the protein and is strongly associated with its correlation time (τ_c) [13]. Therefore, the heteronuclear NOE experiment has been essential to traditional dynamics analyses in conjunction with R_1 and R_2 values. The importance of the NOE is strengthened by the fact that, at the expense of precise R_1 measurements, only precise NOE and R_2 values are necessary to calculate a reliable S^2 [14]. Additionally, the NOE is more sensitive than the R_1 parameter for capturing internal dynamics [10]. The significance of the NOE to the understanding of fast protein dynamics is considerable and we present further evidence to substantiate the use of NOE data for

* Corresponding author. University of Nebraska-Lincoln, Department of Chemistry, 722 Hamilton Hall, Lincoln, NE 68588-0304, USA.
E-mail address: rpowers@unl.edu (R. Powers).

https://doi.org/10.1016/j.ab.2017.11.012
Received 30 June 2017; Received in revised form 24 October 2017; Accepted 18 November 2017
Available online 21 November 2017
0003-2697/

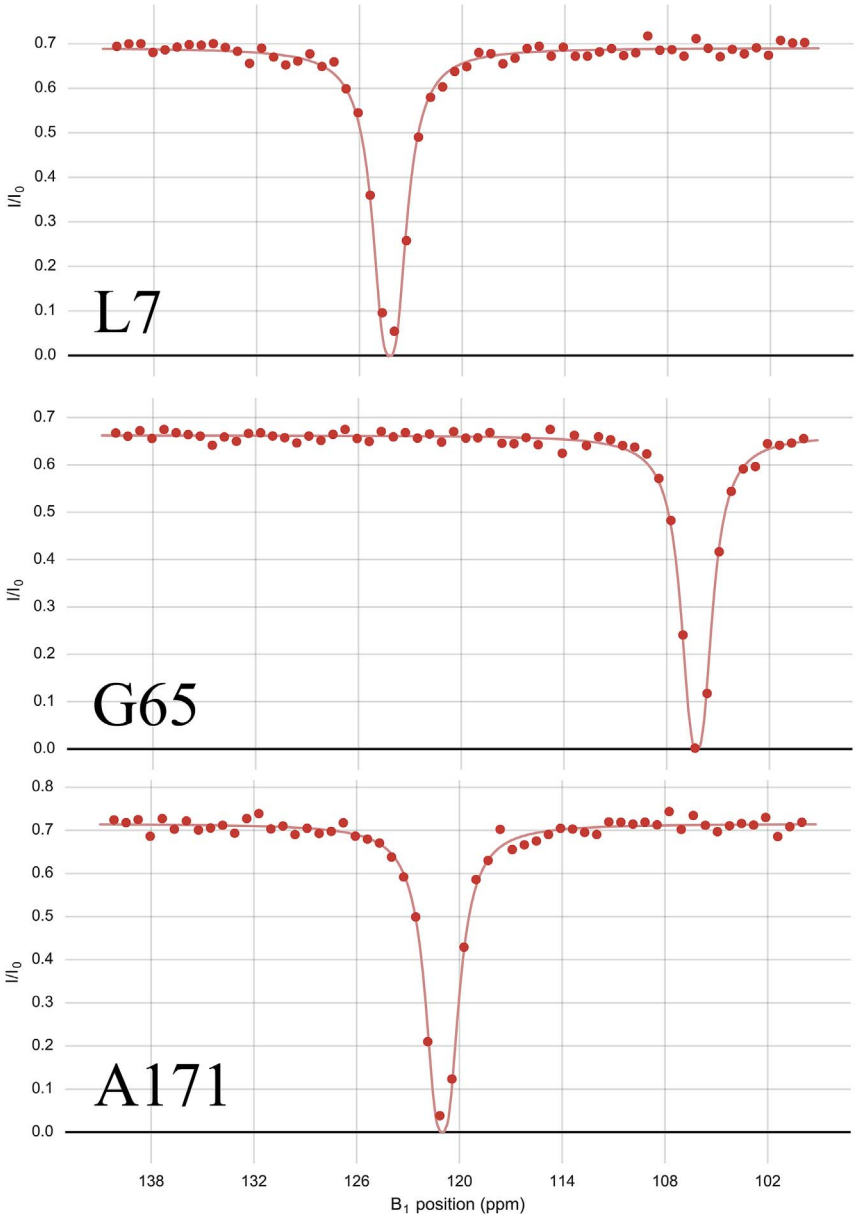

Fig. 1. Representative CEST profiles for 3 residues in DJ-1 Cys106-SH at 35 °C. The profiles show the proper fitting of the dip in intensity and the lack of a noticeable minor state conformation. Residues were chosen based on position in the primary sequence to highlight the consistency of the fitting of the profiles.

Table 1
Average R_1, R_2, NOE, and S^2 values from DJ-1 Cys106-SH at 35 °C.

Exp. Type	Protein	Observed R_1[a]	R_1 Error[b]	Observed R_2[a]	R_2 Error[b]	Observed NOE[a]	NOE Error[b]	Calculated S^2[a]	S^2 Error[b]
Traditional (35 °C)	DJ-1, Cys106-SH	0.78 (0.10)	0.06	19.30 (2.30)	0.7	0.79 (0.11)	0.15	0.92 (0.10)	0.02
CEST (35 °C)	DJ-1, Cys106-SH	0.72 (0.21)	0.06	19.33 (3.50)	2.1	0.79 (0.15)	0.11	0.88 (0.12)	0.07

[a] Standard deviations are in parenthesis.
[b] The reported errors are the standard error of the mean.

Table 2
Average R_1, R_2, NOE, and S^2 values from different physiological states of DJ-1.

Exp. Type	Protein	Observed R_1[a]	R_1 Error[b]	Observed R_2[a]	R_2 Error[b]	Observed NOE[a]	NOE Error	Calculated S^2[a]	S^2 Error[b]
CEST (37 °C)	DJ-1, Cys106-SH	0.72 (0.22)	0.06	19.50 (3.46)	2.1	0.79 (0.16)	0.11	0.86 (0.15)	0.07
	DJ-1, Cys106-SO_2^-	0.78 (0.13)	0.08	20.65 (2.66)	1.3	0.80 (0.16)	0.14	0.92 (0.13)	0.04
	DJ-1, Cys106-SO_3^-	0.71 (0.21)	0.06	18.47 (4.96)	1.0	0.64 (0.42)	0.10	0.76 (0.22)	0.04

[a] Standard deviations are in parenthesis.
[b] The reported errors are the standard error of the mean.

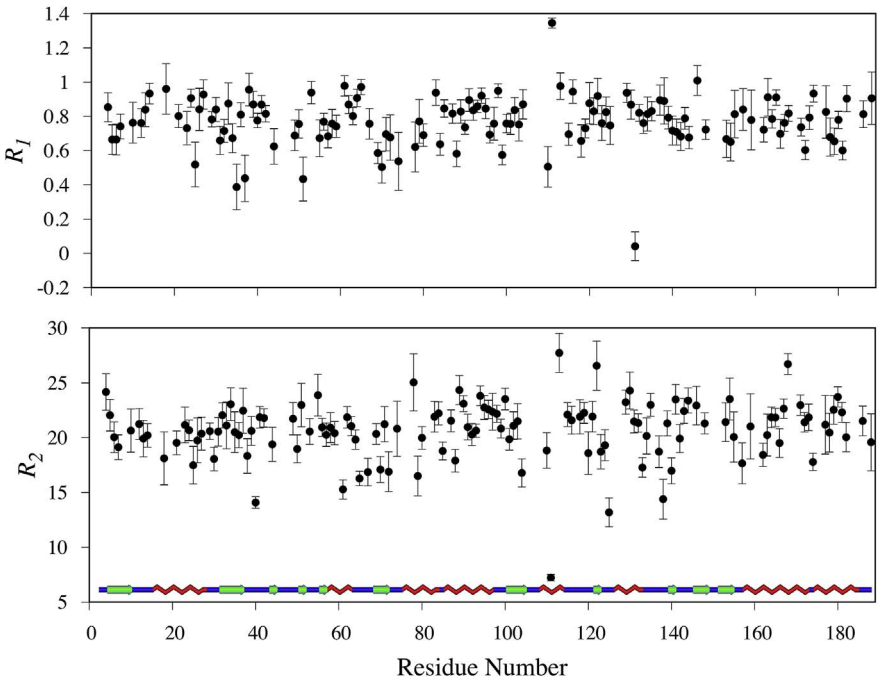

Fig. 2. A plot of the CEST derived R_1 and R_2 parameters for DJ-1 Cys106-SH at 35 °C. The cartoon [6] represents the secondary structure of DJ-1 with helices in red, strands in green, and loops and disordered regions in blue. (For interpretation of the references to colour in this figure legend, the reader is referred to the web version of this article.)

Table 3
RMSD values comparing traditionally collected and CEST datasets for DJ-1 Cys106-SH at 35 °C.

	R_1	R_2	S^2
Traditional vs CEST	0.18	1.95	0.02

modelfree analysis using ^{15}N-CEST experiments.

Material and methods

NMR was used to investigate the dynamics of three DJ-1 oxidation states of Cys106 corresponding to a reduced form (DJ-1 Cys106-SH), a sulfinic acid form (DJ-1 Cys106-SO_2^-) and a sulfonic acid form (DJ-1 Cys106-SO_3^-). The reduced DJ-1 Cys106 was oxidized to a cysteine sulfinic acid by adding hydrogen peroxide at a molar ratio of 1:7 and incubating on ice for 45 min. Similarly, the Cys106 sulfonic acid was prepared by adding hydrogen peroxide at a molar ratio of 1:100 and incubation at room temperature for 2.5 h. Following incubation, the protein was subjected to a buffer exchange to remove excess hydrogen peroxide. All NMR experiments were collected at 37 or 35 °C on a 700 MHz Bruker Avance III spectrometer equipped with a 5 mm QCI-P probe with cryogenically cooled carbon and proton channels. ^{15}N CEST experiments were performed as previously described [7] with B_1 field strengths of 12.5 and 25 Hz. The external field was scanned across the range of 100–140 ppm at a step size of 50 Hz (35 °C) or 25 Hz (37 °C). An interscan delay of 1.5s was employed and ^{15}N saturation was applied for 0.5s. For each experiment a total of 4 transients were collected per 2D plane resulting in a total experiment time of approximately 7 h. Processing was accomplished with NMRPipe [15] and CEST profiles were fit with ChemEx (Fig. 1) [7].

The fitting of the CEST profiles by ChemEx produces R_1 and R_2 relaxation parameters as standard output and is explained in detail in Ref. [7]. The R_1, R_2, NOE, and S^2 errors reported in Tables 1 and 2 were calculated as the standard error of the mean. Heteronuclear NOE experiments were performed as previously described [16] and processed in NMRPipe. FAST-ModelFree analysis was done identical to our previous study to ensure a proper comparison of the methods [16].

Results and Discussion

The fast protein dynamics of reduced DJ-1 have been previously determined using traditional spin relaxation derived R_1 and R_2 values and ^{1}H-^{15}N NOE data [16]. DJ-1 was found to be fairly rigid in solution at 35 °C, with most order parameters (S^2) approaching the maximum theoretical limit ($S^2 = 1$). Importantly, the previous dynamics finding from these traditional relaxation experiments was reproduced with the R_1 and R_2 values obtained from fitting of ^{15}N CEST profiles and from ^{1}H-^{15}N NOE data (Table 1, Fig. 2). Per residue CEST profiles were reliably fit simultaneously for both external fields, although only one field was necessary (Fig. 1). Unfortunately, the fitting of the CEST profiles did not reveal the presence of a minor state or chemical exchange, but this finding did not negatively affect the quality of the derived relaxation parameters. Our results further establish the robustness of the ^{15}N CEST experiment and justify its adoption as an alternative to traditional relaxation experiments. The observed consistency between two distinct sets of R_1, R_2 and S^2 values substantiates previous claims that CEST data is equivalent to traditional spin relaxation experiments [1]. The calculated RMSD values (Table 3) comparing the CEST and traditional R_1 and R_2 values are within the observed standard deviations for the data sets (Tables 1 and 2). An NOE RMSD of 0.13 was obtained when we compared our original ^{1}H-^{15}N NOE data [16] with an NOE data set recollected with the CEST experiments. Again, the NOE RMSD is within the observed experimental error and standard deviations (Tables 1 and 2).

The per residue delta plots of the R_1, R_2 and S^2 values shown in Fig. 3 further illustrates the consistency between the two methods. The low variability in the R_2 delta plot indicates that the CEST profile linewidths were robust in the reporting of the true R_2 values and that there was an absence of chemical exchange. Only a slight overall difference of the methods was observed based on an S^2 RMSD of 0.02. This is despite the fact that the prior dynamics measurements were carried out on different NMR spectrometers at different field strengths (*i.e.,* 500 MHz vs. 700 MHz). The largest variations in the observed ΔS^2 values were primarily located in loop regions, which are expected to be more sensitive to subtle temperature and solvent differences. A few residues with large ΔS^2 were removed from the comparison since the ΔS^2 error was likely a result of peak overlap and not representative of the overall quality of the CEST data. It is again important to note that

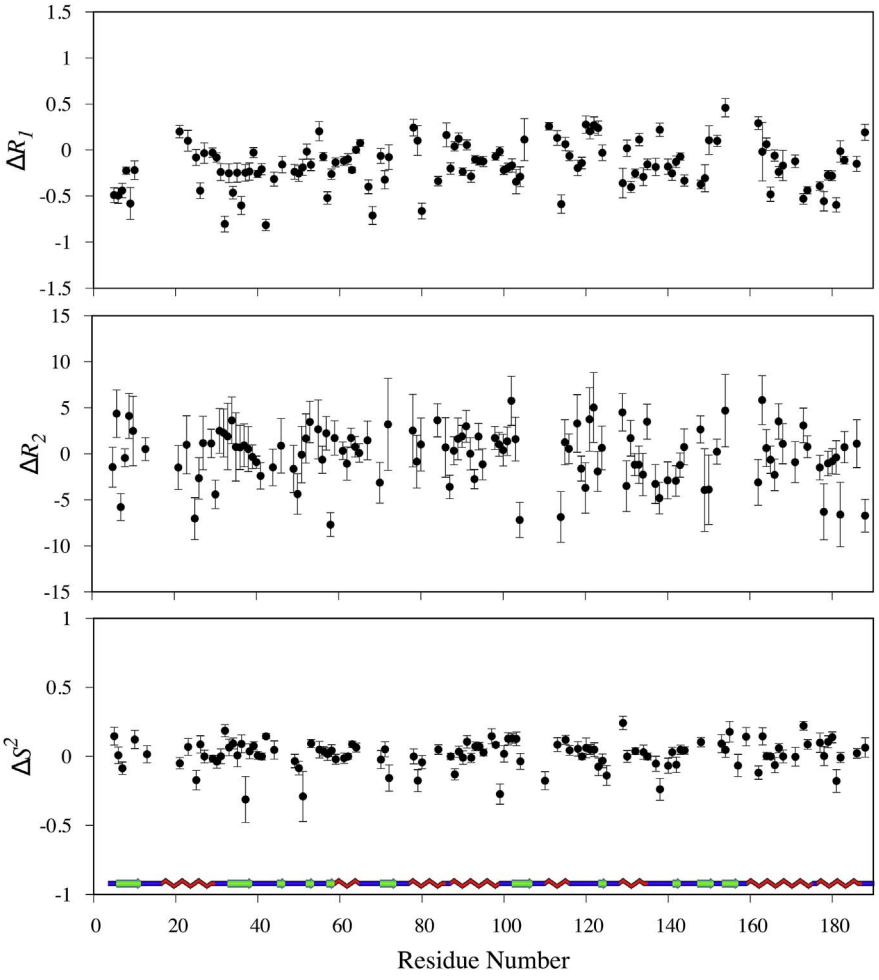

Fig. 3. A delta plot of the R_1, R_2, and generalized order parameters comparing traditionally collected data versus CEST derived data for DJ-1 Cys106-SH at 35 °C. The cartoon [6] represents the secondary structure of DJ-1 with helices in red, strands in green, and loops and disordered regions in blue. (For interpretation of the references to colour in this figure legend, the reader is referred to the web version of this article.)

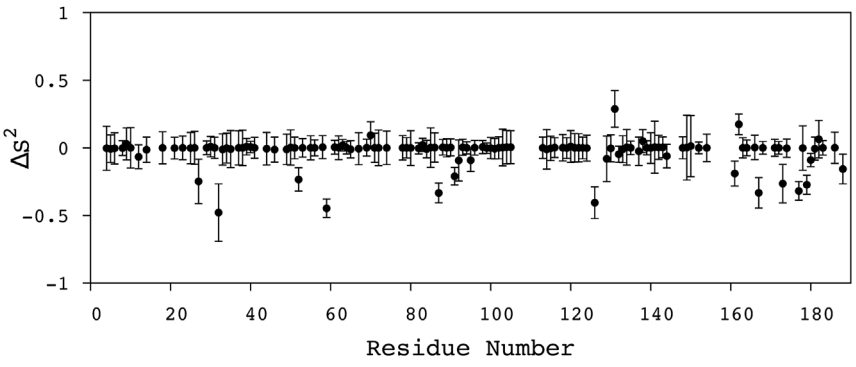

Fig. 4. A delta plot of the generalized order parameters comparing DJ-1 Cys106-SH and DJ-1 Cys106-SO_3^- NOE data. Data points below zero indicate an increase in internal motion due to the DJ-1 Cys106-SO_3^- NOE value.

these datasets were collected several years apart on different protein samples, on different spectrometers, and by different spectroscopists. Therefore, although the reproducibility between the two datasets is not on par with prior results [1], our comparison does represent a more realistic scenario and a more accurate representation of the true uncertainty. Importantly, the final results of the modelfree analyses from both the CEST and CPMG datasets led to the same conclusions regarding the overall dynamic properties of DJ-1.

Leveraging the ^{15}N-CEST experiment, several naturally occurring oxidation states of DJ-1 were studied (Cys106-SH, -SO_2^-, -SO_3^-) to identify if there were any differences in their dynamic properties. At physiological temperature (37 °C), none of the three forms of DJ-1 exhibited a minor state conformer based on analysis of the CEST profiles. The CEST-derived R_1 and R_2 parameters for each of the DJ-1 states were further analyzed to identify any ps-ns timescale dynamics that may differ between the three states. Interestingly, there were only minor differences in the R_1 and R_2 relaxation parameters between the three states in addition to being comparable to our previous results (Tables 1 and 2). ^{1}H-^{15}N NOE experiments were subsequently performed to further explore the dynamic properties of the three DJ-1 states. A drastic change was readily apparent in DJ-1 Cys106-SO_3^-, where the average NOE is lower, and the NOE standard deviation is much larger compared to the two other DJ-1 states (Table 2). The CEST derived R_1 and R_2 parameters and the heteronuclear NOE values were then used with FAST-ModelFree [17–19] to determine the per residue order parameters. The dynamic properties for the first two DJ-1 states are quite similar to our previously published results for the reduced form of DJ-1, where the protein exhibits minimal motion on the ps-ns time scale. Conversely, DJ-1 Cys106-SO_3^- exhibits a significant increase in dynamics based on an overall lower S^2 value of 0.76 ± 0.22.

Importantly, it appears that the main contributor to the increase in dynamics for DJ-1 Cys106-SO_3^- is a reduction in the average NOE from approximately 0.80 to 0.64 ± 0.42. Further, it is well known that NOE data is essential for the accurate analysis of protein dynamics since the NOE is very sensitive to fast internal dynamics (e.g., τ_e), as previously defined in Kay et al. (1989) [10]. In addition, the large standard deviation in the NOEs for DJ-1 Cys106-SO_3^- is also indicative of a substantial decrease in structural stability. This is consistent with the observation that DJ-1 Cys106-SO_3^- was less stable than the other two forms of the protein. DJ-1 Cys106-SO_3^- would aggregate and precipitate out of solution after approximately two days at 37 °C. Conversely, the reduced and sulfinic forms of DJ-1 were indefinitely stable.

To gain insight on the impact of the NOEs on the per residue order parameters, the NOE data from DJ-1 Cys106-SO_3^- was combined with the R_1 and R_2 data from DJ-1 Cys106-SO_2^-. DJ-1 Cys106-SO_2^- is arguably the most rigid form of DJ-1 since it has the highest average order parameter of 0.92 ± 0.13. Moreover, DJ-1 Cys106-SO_2^- has the lowest R_1 and R_2 standard deviations of 0.13 and 2.66, respectively. Any changes in the order parameters calculated by combining the DJ-1 Cys106-SO_2^- R_1 and R_2 data with the DJ-1 Cys106-SO_3^- NOE data will highlight the impact of the more dynamic NOEs on the calculated order parameters. Fig. 4 shows the ΔS^2 obtained from comparing the DJ-1 Cys106-SH and Cys106-SO_3^- NOE data. It is readily apparent that the more dynamic NOEs contribute significantly to the per residue order parameters as approximately 10 residues order parameters decreased by −0.25 or more. These differences are noteworthy because they may change the classification of a residue from “ordered” to “disordered”. Interestingly, a majority of the ΔS^2 values are near zero, which indicates essentially identical dynamics between the two states. Not surprisingly, only the residues with a significant difference in NOE values were substantially affected. It is likely that these DJ-1 residues in the Cys106-SO_3^- form have sub-ns internal motions, which make them sensitive to the ^{1}H-^{15}N NOE experiment. These findings are significant because exclusion of any NOE data would have hidden the true dynamics of these particular DJ-1 residues.

Conclusion

The purpose of this study was to further evaluate the robustness of the ^{15}N CEST experiments as an alternative method to determine the fast protein dynamics of three physiological states of DJ-1 while combining CEST derived R_1 and R_2 parameters with traditional NOE values. Initial results confirmed that this new method was comparable to traditional dynamics analyses as our results correspond well with previous findings. We have also reaffirmed the importance of the heteronuclear NOE to dynamics analysis. Extremely low NOE values are strong indicators of protein disorder or unfolding and, in this study, were the only experimental evidence for this phenomenon in DJ-1 since the R_1 and R_2 parameters were similar for the three DJ-1 states. To our knowledge, this is the first study that combines ^{15}N CEST data with a traditional model-free analysis of a biological system and also confirms the necessity of NOE data for exploring fast protein dynamics.

Contributions

AJL, JC, JL, NMM, and TA performed the experiments; JC, RP, TA, and MW designed the experiments, analyzed the data and wrote the manuscript.

Acknowledgments

The authors would like to thank Drs. Martha Morton and Joseph Dumais of the Research Instrumentation Facility in the Department of Chemistry at UNL for assistance with data collection and suggestions. The manuscript was supported in part by funds from the National Institutes of Health (NIH) grant R01-GM092999; the Molecular Mechanisms of Disease Pre-doctoral training grant (T32-GM107001, NIGMS); the Redox Biology Center (P30 GM103335, NIGMS); and the Nebraska Center for Integrated Biomolecular Communication (P20-GM113126, NIGMS). The research was performed in facilities renovated with support from the National Institutes of Health (RR015468-01).

References

[1] Y. Gu, A.L. Hansen, Y. Peng, R. Bruschweiler, Rapid determination of fast protein dynamics from NMR chemical exchange saturation transfer data, Angew. Chem. Int. Ed. Engl. 55 (2016) 3117–3119.
[2] A.G. Palmer, C.D. Kroenke, J. Patrick Loria, Nuclear magnetic resonance methods for quantifying microsecond-to-millisecond motions in biological macromolecules, Proteins 339 (2001) 204–238.
[3] L.E. Kay, New views of functionally dynamic proteins by solution NMR spectroscopy, J. Mol. Biol. 428 (2016) 323–331.
[4] G. Lipari, A. Szabo, Model-free approach to the interpretation of nuclear magnetic resonance relaxation in macromolecules. 1. Theory and range of validity, J. Am. Chem. Soc. 104 (1982) 4546–4559.
[5] G.M. Clore, A. Szabo, A. Bax, L.E. Kay, P.C. Driscoll, A.M. Gronenborn, Deviations from the simple two-parameter model-free approach to the interpretation of Nitrogen-15 nuclear magnetic relaxation of proteins, J. Am. Chem. Soc. 112 (1990) 4989–4991.
[6] M. Tollinger, N.R. Skrynnikov, F.A.A. Mulder, J.D. Forman-Kay, L.E. Kay, Slow dynamics in folded and unfolded states of an SH3 domain, J. Am. Chem. Soc. 123 (2001) 11341–11352.
[7] P. Vallurupalli, G. Bouvignies, L.E. Kay, Studying “invisible” excited protein states in slow exchange with a major state conformation, J. Am. Chem. Soc. 134 (2012) 8148–8161.
[8] N.L. Fawzi, J. Ying, R. Ghirlando, D.A. Torchia, G.M. Clore, Atomic-resolution dynamics on the surface of amyloid-beta protofibrils probed by solution NMR, Nature 480 (2011) 268–272.
[9] N.J. Anthis, G.M. Clore, Visualizing transient dark states by NMR spectroscopy, Q. Rev. Biophys. 48 (2015) 35–116.
[10] L.E. Kay, D.A. Torchia, A. Bax, Backbone dynamics of proteins as studied by 15N inverse detected heteronuclear NMR spectroscopy: application to staphylococcal nuclease, Biochemistry 28 (1989) 8972–8979.
[11] A. Abragam, The Principles of Nuclear Magnetism, Clarendon Press, Oxford, 1961.
[12] P. Valluruapalli, A. Sekhar, T. Yuwen, L.E. Kay, Probing conformational dynamics in biomolecules via chemical exchange saturation transfer: a primer, J. Biomol. NMR 67 (2017) 243–271.
[13] D. Gust, R.B. Moon, J.D. Roberts, Applications of natural-abundance nitrogen-15 nuclear magnetic resonance to biochemically important molecules, Proc. Natl. Acad. Soc. U. S. A. 72 (1975) 4696–4700.
[14] D. Jin, M. Andrec, G.T. Montelione, R.M. Levy, Propagation of experimental uncertainties using the Lipari-Szabo model-free analysis of protein dynamics, J. Biomol. NMR 12 (1998).
[15] F. Delaglio, S. Grzesiek, G.W. Vuister, G. Zhu, J. Pfeifer, A. Bax, NMRPipe: a multidimensional spectral processing system based on UNIX pipes, J. Biomol. NMR 6 (1995) 277–293.
[16] N.M. Milkovic, J. Catazaro, J. Lin, S. Halouska, J.L. Kizziah, S. Basiaga, R.L. Cerny, R. Powers, M.A. Wilson, Transient sampling of aggregation-prone conformations causes pathogenic instability of a parkinsonian mutant of DJ-1 at physiological temperature, Protein Sci. 24 (2015) 1671–1685.
[17] A.G. Palmer, M. Rance, P.E. Wright, Intramolecular motions of a zinc finger DNA-binding domain from xfin characterized by proton-detected natural abundance 13C heteronuclear NMR spectroscopy, J. Am. Chem. Soc. 113 (1991) 4372–4380.
[18] A.M. Mandel, M. Akke, A.G. Palmer, Backbone dynamics of Escherichia coli ribonuclease HI: correlations with structure and function in an active enzyme, J. Mol. Biol. 246 (1995) 144–163.
[19] R. Cole, J.P. Loria, FAST-ModelFree: a program for rapid automated analysis of solution NMR spin-relaxation data, J. Biomol. NMR 26 (2003) 203–213.